

Oxygenation Mechanism of Ribulose-Bisphosphate Carboxylase/Oxygenase. Structure and Origin of 2-Carboxytetritol 1,4-Bisphosphate, a Novel O₂-Dependent Side Product Generated by a Site-Directed Mutant[†]

Mark R. Harpel,^{*,‡} Engin H. Serpersu,[§] John A. Lamerdin,[§] Zhi-Heng Huang,^{||} Douglas A. Gage,^{||} and Fred C. Hartman^{*,‡}

Protein Engineering Program, Biology Division, Oak Ridge National Laboratory, Oak Ridge, Tennessee 37831, Department of Biochemistry, University of Tennessee, Knoxville, Tennessee 37996, and Mass Spectrometry Facility, Department of Biochemistry, Michigan State University, East Lansing, Michigan 48824

Received April 14, 1995; Revised Manuscript Received June 20, 1995[®]

ABSTRACT: Site-directed mutagenesis has implicated active-site Lys329 of *Rhodospirillum rubrum* ribulose-1,5-bisphosphate carboxylase/oxygenase (Rubisco) in promoting the reaction of CO₂ with the 2,3-enediol of ribulose bisphosphate and in stabilizing carboxylation intermediates [Hartman, F. C., & Lee, E. H. (1989) *J. Biol. Chem.* 264, 11784–11789; Lorimer, G. H., Chen, Y.-R., & Hartman, F. C. (1993) *Biochemistry* 32, 9018–9024]. Although the K329A mutant is greatly impaired in carboxylation, it catalyzes formation of the enediol, which is misprocessed to an O₂-dependent side product [Harpel, M. R., & Hartman, F. C. (1994) *Biochemistry* 33, 5553–5561]. We now identify this novel side product as 2-carboxytetritol 1,4-bisphosphate (CTBP) by mass spectrometry, ¹H-, ¹³C-, and ³¹P-NMR spectroscopy, and peroxide oxidation. H₂O₂ accumulates during formation of CTBP, which we show to be derived from a transient precursor, the dicarbonyl D-glycero-2,3-pentodiulose 1,5-bisphosphate. The isolated dicarbonyl bisphosphate is processed by K329A to CTBP. These results, combined with isotope-labeling studies, suggest that CTBP arises by H₂O₂ elimination from an improperly stabilized peroxy adduct of the enediol intermediate, followed by rearrangement of the resulting dicarbonyl. Therefore, normal oxygenation, as catalyzed by wild-type Rubisco, is not a spontaneous reaction but must involve stabilization of the peroxy intermediate to mitigate formation of the dicarbonyl bisphosphate and subsequently CTBP. CTBP formation verifies the identity of Rubisco's previously invoked oxygenase intermediate, provides additional mechanistic insight into the oxygenation reaction, and shows that Lys329 promotes oxygenation as well as carboxylation. These results may be relevant to other oxygenases, which also exploit substrate carbanions rather than organic cofactors or transition metals for biological oxygen utilization.

Rubisco¹ must catalyze at least five chemically distinct partial reactions and stabilize multiple intermediates and transition states to accomplish its physiological role, the carboxylation of RuBP to form two molecules of PGA. These demands likely account for the enzyme's catalytic imperfec-

tions; apart from its low turnover number (2–5 s⁻¹), Rubisco catalyzes several side reactions, which mitigate productive substrate throughput and negatively impact the metabolic efficiency of photosynthetic organisms [for reviews, see Hartman and Harpel (1993, 1994), Andrews et al. (1994), Schloss (1990), and Andrews and Lorimer (1987)].

The undesirable activity of Rubisco that has received the greatest attention is the oxidative cleavage of RuBP, whereby utilization of O₂ as a cosubstrate instead of CO₂ forms 1 equiv each of PGA and PGyc (Bowes et al., 1971; Lorimer et al., 1973). This activity presents a mechanistically intriguing problem: Rubisco acts as a mixed-function oxygenase in the absence of cofactors or transition metals traditionally associated with biological oxygen activation. Although the carboxylation and oxygenation pathways follow similar reaction coordinates and utilize a common enediol intermediate (Pierce et al., 1986; Lorimer & Andrews, 1973; Andrés et al., 1993), the means for discrimination between CO₂ and O₂ addition by Rubisco is unclear. In particular, a carboxyketone intermediate of the carboxylase reaction (Figure 1A) has been isolated and characterized (Pierce et al., 1986), but a corresponding peroxyketone intermediate of the oxygenase reaction (Figure 1B) has only been postulated (Lorimer et al., 1973; Lorimer, 1981; Mizioro & Lorimer, 1983).

[†] This research was sponsored by the Office of Health and Environmental Research, United States Department of Energy, under contract DE-AC05-84OR21400 with Martin Marietta Energy Systems, Inc. (to F.C.H. and M.R.H.), Grant GM42661 from the National Institute of General Medical Science (to E.H.S.), and Grant RR00480 from the Biotechnology Research Technology Program, National Center for Research Resources, National Institute of Health (to D.A.G.).

[‡] Oak Ridge National Laboratory.

[§] University of Tennessee.

^{||} Michigan State University.

[®] Abstract published in *Advance ACS Abstracts*, August 15, 1995.

¹ Abbreviations: Rubisco, D-ribulose 1,5-bisphosphate carboxylase/oxygenase (EC 4.1.1.39); RuBP, D-ribulose 1,5-bisphosphate; K329A, mutant of Rubisco in which lysyl at position 329 has been replaced by alanyl by site-directed mutagenesis; bicine, N,N-bis(2-hydroxyethyl)-glycine; PGA, 3-phospho-D-glycerate; PGyc, 2-phosphoglycolate; CTBP, 2-carboxytetritol 1,4-bisphosphate; SDS, sodium dodecyl sulfate; PAGE, polyacrylamide gel electrophoresis; GC-MS, gas chromatography–mass spectrometry; TMS-, trimethylsilyl; ESI-MS, electrospray ionization mass spectrometry; COSY, two-dimensional correlation spectroscopy; TOCSY, total correlation spectroscopy; INEPT, insensitive nuclei spectroscopy enhanced by polarization transfer; CABP, 2-carboxy-D-arabinitol 1,5-bisphosphate; XuBP, D-xylulose 1,5-bisphosphate; DHAP, dihydroxyacetone phosphate; HRP, horseradish peroxidase; ABTS, 2,2'-azino-bis(3-ethylbenzthiazoline-6-sulfonic acid); PIPES, piperazine-N,N-bis(2-ethanesulfonic acid).

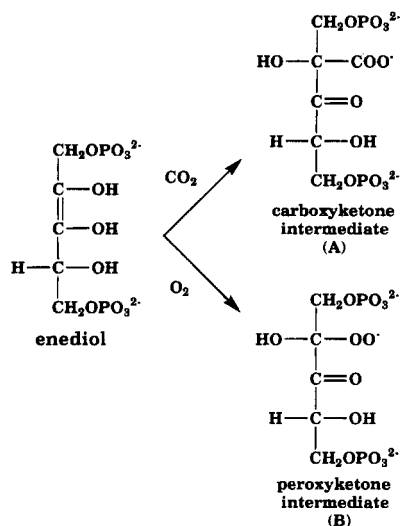


FIGURE 1: Carboxyketone (A) and putative peroxyketone (B) intermediates of the carboxylation and oxygenation reactions catalyzed by Rubisco.

Oxygenation of simple organics is hindered by the necessity to conserve net spin angular momentum in the spin-forbidden interaction between triplet O₂ and singlet organic molecules. The traditional view of biological oxygenation has been limited to transition metals to overcome the spin barrier or conjugated organic cofactors to stabilize radical intermediates (Hamilton, 1974). Recent work has shown that other enzymes, independent of these cofactors, also initiate O₂ activation via carbanionic intermediates (Abell & Schloss, 1991; Wray & Abeles, 1995). Such enzymes stabilize intermediate substrate- and oxygen-radicals for recombination (Lorimer, 1981) and/or induce intersystem crossover for substrate spin inversion, which could theoretically be rendered thermally accessible by geometric perturbation of the carbanion (Andrés et al., 1993). Formation of an oxygenation intermediate could thus depend upon both accessibility of O₂ to the carbanion and inducement of the correct spatial and electronic conformation of the carbanion for reaction with O₂. Successful forward processing of the resulting peroxy adduct, regardless of how formed, ultimately depends upon its stabilization by the enzyme through metal ligation or protonation (Abell & Schloss, 1991).

Studies of active-site Lys329² of Rubisco have been particularly informative with regard to the chemistry of addition of CO₂ and O₂ to the RuBP enediol. On the basis of crystallography (Andersson et al., 1989; Knight et al., 1990; Schreuder et al., 1993; Newman & Gutteridge, 1993), Lys329 stabilizes the closed conformation of a flexible loop (loop 6) through ionic bonds with both active-site Glu48 (from the flexible N-terminal segment of the adjacent subunit) and the carboxylate group, which mimics substrate CO₂, of bound CABP, an analog of the carboxylated intermediate. In this conformation, loop 6 helps to sequester the active site from solvent and to prevent dissociation of reaction intermediates (Larson et al., 1995).

Functional analyses provide evidence that Lys329 plays a primary role in catalyzing CO₂ addition to the enediol of RuBP. Specifically, position-329 mutants are nearly devoid of carboxylation activity and are unable to form stable

complexes with CABP (Soper et al., 1988), but they retain activity in both enolization of RuBP (Hartman & Lee, 1989) and hydrolysis of isolated carboxyketone reaction intermediate (Lorimer et al., 1993). Substitution at position 329 by lysyl analogs (introduced by covalent or noncovalent chemical rescue of Lys329 mutants) results in restored carboxylation activities but reduced CO₂/O₂ specificities (Smith & Hartman, 1988; Lorimer et al., 1993; Harpel & Hartman, 1994). Arginyl substitution also drastically reduces carboxylation specificity (Gutteridge et al., 1993). Hence, precise positioning of the Lys329 ε-amino group is important for preferential stabilization of the transition state for carboxylation versus oxygenation.

We have recently shown that the K329A mutant slowly processes RuBP enediol to two major side products (Harpel & Hartman, 1994). Because its formation is dependent on O₂, one of these aberrant products, designated "X" in our prior communication, provides an entree into the mechanism of O₂ utilization by Rubisco. Chemical rescue of K329A by ethylamine restores normal conversion of RuBP to PGA and PGyc and eliminates conversion to the side products. Hence, X arises from misprocessing of a reaction intermediate, presumably along the oxygenase pathway.

In this study, we establish the structure of X as 2-carboxytetritol 1,4-bisphosphate (CTBP) and elucidate the pathway for its formation. Our findings provide new mechanistic insight into Rubisco's oxygenation reaction and further our understanding of roles of Lys329 in stabilizing reaction intermediates and assisting in gaseous substrate addition.

EXPERIMENTAL PROCEDURES

Materials. RuBP [unenriched (Horecker et al., 1958) or 1-³H-, 5-³H-, 2-¹³C-, and U-¹³C-labeled (Kuehn & Hsu, 1978)] and [¹⁴C-carboxy]CABP (Pierce et al., 1980), used as an epimeric mixture of the *arabino* and *ribo* isomers, were synthesized and purified according to the published protocols. RuBP concentrations were determined by the enzyme-coupled spectrophotometric assay for PGA produced by wild-type Rubisco (Schloss et al., 1982). 2-³H- and 6-³H-labeled glucose were purchased from ICN; 3-¹³C- and U-¹³C-labeled glucose were purchased from Cambridge Isotope Laboratories at 99 and >98 atom-% purity, respectively. The positions of isotope enrichment in synthesized 2-¹³C- and U-¹³C-labeled RuBP were verified by ¹³C NMR.

Wild-type *Rhodospirillum rubrum* Rubisco was prepared as described (Schloss et al., 1982). The mutated *R. rubrum* *rbc* gene encoding K329A Rubisco (Soper et al., 1988) was overexpressed in *Escherichia coli* strain MV1190 from a derivative of vector pFL245 (Larimer et al., 1990). As previously described, the K329A protein was purified to homogeneity (Harpel et al., 1991; Harpel & Hartman, 1994) as judged by Coomassie Blue staining of SDS-PAGE gels. Phosphoribulokinase used in the synthesis of RuBP was purified from spinach leaves (Porter et al., 1988). All other enzymes were obtained from Sigma Chemical Co.

Protein and Activity Assays. Concentrations of Rubisco proteins were determined from the absorbancy at 280 nm [1.2 AU for 1 mg/mL; (Schloss et al., 1982)].

Turnover products from ³H-labeled RuBP were analyzed by radiometric anion-exchange chromatography (Harpel et al., 1993). Deproteinized reaction mixtures were applied to a column of Mono Q anion-exchanger (Pharmacia HR 5/5,

² All residue numbers refer to the sequence position in *Rhodospirillum rubrum* Rubisco.

5 mm \times 50 mm) and eluted with a gradient of NH_4Cl at pH 8.0, depicted in Figure 7D, in the presence of 10 mM sodium borate.

Synthesis and Isolation of Reaction Side Product. Large-scale synthesis of CTBP was carried out under a 100% O_2 atmosphere to maximize product yield. A typical preparative reaction mixture (pH 8) contained 50 mM bicine, 10 mM MgCl_2 , 1 mM EDTA, 3.6 mM NaHCO_3 , 10% (v/v) glycerol, 1.3 mg/mL K329A, and 1.3 mM RuBP in a volume of 10 mL. $[1\text{-}^3\text{H}]\text{RuBP}$ (2000–5000 cpm/ μmol) was included to provide chromatographic markers. The reactions were carried out at room temperature in a 25 mL conical side-arm flask linked to O_2 flow through a gas adapter. The reaction solvent (all components except RuBP and K329A) was sparged with 100% O_2 for 3–4 h and then introduced into the O_2 -purged reaction flask. Neutralized RuBP was next added under constant O_2 flow through the open side arm. After 15 min, K329A was introduced to initiate the reaction. The vessel was then flushed with O_2 for an additional 15 min and sealed under slightly positive pressure. After being stirred for 15 h at 23 $^\circ\text{C}$, the reaction was quenched with 19 mM sodium borohydride to reduce the remaining RuBP, followed 15 min later by 41 mM glucose. Quenching by borohydride does not affect CTBP, as deduced from the lack of radiolabel incorporation into CTBP from $\text{NaB}[^3\text{H}]_4$ (Harpel & Hartman, 1994) and from an unaltered anion-exchange elution position following reductive quenching (data not shown).

After removal of protein from the quenched reaction by ultrafiltration (Amicon Centricon-10), CTBP was purified by anion-exchange chromatography. The reaction was processed in two batches by diluting each to 10 mL with H_2O , loading onto a Mono Q HR 5/5 column, and eluting with a stepwise gradient of NH_4HCO_3 at pH 8 (25 mM isocratic elution for 4 mL, followed by gradients of 25–85 mM over 6 mL, 85–150 mM over 5 mL, 150–225 mM over 22 mL, and 225–500 mM over 10 mL). Fractions (0.5 mL) were collected. CTBP-containing fractions (eluting at \sim 225 mM NH_4HCO_3) from the two runs were combined and lyophilized to dryness. The residue was dissolved in 10 mL of distilled water and re-lyophilized to remove excess NH_4HCO_3 ; this process was repeated several times. The final solution, containing \sim 1 μmol of CTBP in 1 mL, was stored at -80°C . Samples for ^1H -NMR were lyophilized an additional 3–4 times from D_2O . ^{13}C -enriched CTBP was prepared from $U\text{-}^{13}\text{C}$ - and $2\text{-}^{13}\text{C}$ -labeled RuBP under identical conditions. In rechromatography on Mono Q, isolated CTBP co-eluted with the peak observed in analytical reactions.

Dephosphorylated CTBP was prepared from the purified ammonium salt of CTBP (2–5 mM) by overnight hydrolysis at 23 $^\circ\text{C}$ and pH 8 with 20–25 units/mL *E. coli* alkaline phosphatase. Following deproteination (Amicon Minicon-30), the dephosphorylated compound was isolated from buffer components and inorganic phosphate by isocratic elution (2 mM NH_4HCO_3 at pH 8) from Mono Q. Fractions containing the dephosphorylated compound (eluting as a -1 charged species) were pooled and lyophilized.

Mass Spectrometry. GC-MS analyses of dephosphorylated CTBP, derivatized at 60 $^\circ\text{C}$ for 30 min with bis[TMS]-*N*-trifluoroacetamide (BSTFA) that contained 1% trimethylchlorosilane (TMCS) (Regis Chemical Co.), were performed with a Hewlett-Packard GC5890 chromatograph equipped with a DB-1701 GC column (J & W Scientific, 15 m \times 0.25

mm \times 0.25 μm film thickness) interfaced via a heated inlet to a JEOL JMS-AX505H mass spectrometer. A temperature gradient of 10 $^\circ\text{C}/\text{min}$ from 100 to 300 $^\circ\text{C}$ was used for GC. MS entailed electron impact at 30 eV; ions were detected in positive-ion mode.

NMR Spectroscopy. NMR spectra were collected at 300 K with a wide-bore Bruker AMX 400 spectrometer. Samples (1.5–3 mM) were prepared in D_2O at pH \sim 8, except for the sample used for the COLOC experiment, which was adjusted to pH \sim 5. One-dimensional ^1H NMR spectra were collected over a spectral width of 3205 Hz with 32K data points. Phosphorus and carbon spectra were obtained with proton decoupling over a width of 3247 and 31250 Hz, respectively. Proton, phosphorus, and carbon chemical shifts were referenced to external disodium 2,2-dimethyl-2-silapentane-5-sulfonate, phosphoric acid, and dioxan (67 ppm), respectively.

Nuclear connectivities were established by two-dimensional ^1H – ^1H TOCSY (HOHAHA; MLEV 17 spin lock) and COLOC (Kessler et al., 1984) experiments. For homonuclear correlation experiments, the transmitter offset was placed on the $^2\text{HO}^1\text{H}$ resonance peak, which was irradiated with low power during the relaxation delay. The experiments were carried out using a spectral width of 4424 Hz. Data points (2K) were recorded in t_2 for each of the 92–142 t_1 values, with 128 transients per t_1 increment. TOCSY spectra were recorded with mixing times of 21 and 53 ms, including two 2.5 ms trim pulses. Data were collected in the phase-sensitive mode using the time-proportional phase increment method (Marion & Wüthrich, 1983). The data were then zero-filled to 0.5K points in t_1 and multiplied by a shifted sin or $(\sin)^2$ window function in both dimensions before Fourier transformation. Phase and baseline corrections were performed in both dimensions. The COLOC experiment established three-bond ^1H – C – O – ^{31}P connectivity. Optimal results were obtained by using delays of 28 and 12 ms. The spectra were acquired with a spectral width of 1629 Hz and 2K data points in the F_2 dimension with 128 t_1 increments. In the F_1 dimension, 256 scans were collected for each t_1 over a spectral width of 2400 Hz. The data were zero-filled to 0.5K in the F_1 dimension, and Gaussian–Lorentzian multiplication was applied to the data in both dimensions. Other conditions are stated in the figure legends.

Periodate Oxidation and Identification of Degradation Products. CTBP derived from $1\text{-}^3\text{H}$ - or $5\text{-}^3\text{H}$ -labeled RuBP (denoted $[1\text{-}^3\text{H}]\text{CTBP}$ and $[4\text{-}^3\text{H}]\text{CTBP}$, respectively), was analyzed by oxidative degradation with sodium metaperiodate (see Figure 6). In each case, isolated CTBP (12.5 nmol in 250 μL) was treated with a 15-fold molar excess of periodate in 50 mM phosphate buffer (pH 7.5) for 7.5 h at 23 $^\circ\text{C}$ and then quenched with 20 μL of ethylene glycol. The predominate periodate-cleavage products were identified subsequent to further processing.

The radiolabeled product from oxidation of $[1\text{-}^3\text{H}]\text{CTBP}$ was identified as phosphohydroxypyruvate by successive chemical reduction with sodium borohydride and D-PGA-specific enzymatic reduction with NADH (Schloss et al., 1982). Chemical reduction entailed treatment with 25.5 mM NaBH_4 for 15 min and quenching with 60 mM glucose. An aliquot of this material was then supplemented with 1.4 mM NADH and treated with the appropriate coupling enzymes for 30 min. An epimeric mixture of $[^{14}\text{C}\text{-carboxy}]\text{CABP}$

was oxidized by periodate and treated similarly to provide a structurally related standard.

The radiolabeled oxidation product derived from [4-³H]-CTBP was identified as glycoaldehyde phosphate by aldolase-catalyzed condensation with DHAP to form XuBP. The aldol condensation reaction (pH 6.5) contained 50 mM PIPES, 10 mM MgCl₂, 0.1 mM EDTA, and carrier levels of unlabeled DHAP (4 mM) and glycoaldehyde phosphate (1 mM). The glycoaldehyde phosphate was prepared by acid hydrolysis of the diethylacetal (Calbiochem) at 40 °C for 30 min and neutralization to pH ~5.5 with 0.8 molar equivalent of NaHCO₃. The contributing chemical concentration of [2-³H]glycoaldehyde phosphate product, which was purified from the periodate reaction by Mono Q chromatography, was ~5 μM. Rabbit muscle aldolase, pre-treated with one molar equivalent of iodoacetol phosphate to inactivate contaminating triosephosphate isomerase (Hartman, 1971), was added to 1.1 mg/mL, and the reaction was incubated at 37 °C for 4 h.

XuBP formed in the condensation reaction was identified by its elution position from Mono Q, by product profiles after its reduction with NaBH₄, and by its utilization as a substrate by wild-type *R. rubrum* Rubisco (Lee et al., 1993). Half of the condensation reaction was quenched with 1% (w/v) SDS. Of the other half, one portion was also treated with 1% (w/v) SDS, reduced with NaBH₄ (15 mM), and quenched with glucose (60 mM). The remaining portion was brought to pH 8 with bicine (0.2 M final) and supplemented with 10 mM MgCl₂, 0.5 mM EDTA, 80 mM NaHCO₃, and 2.2 mg/mL wild-type *R. rubrum* Rubisco. After 2.25 h at 23 °C, the Rubisco reaction was stopped with 1% (w/v) SDS. All samples were deproteinized by ultrafiltration and analyzed on Mono Q.

Reaction Time Courses for Product Accumulation by K329A. Product accumulations were monitored by periodically quenching aliquots of [1-³H]RuBP-containing reactions with 1% (w/v) SDS, deproteinizing by ultrafiltration, and analyzing chromatographically for radiolabeled components. The reactions (pH 8) contained 45 mM bicine, 9 mM MgCl₂, 0.5 mM EDTA, 10.5 mM NaHCO₃, 10% (v/v) glycerol, 255 μM O₂, 1.1 mg/mL K329A, and ± 50 mM sodium borate and were initiated with 250 μM [1-³H]RuBP (1.2 × 10⁷ cpm/μmol).

H₂O₂ Detection. H₂O₂ was detected colorimetrically by peroxidase-mediated oxidation of ABTS (Childs & Bardsley, 1975). The ABTS/HRP assay was standardized with stock solutions of H₂O₂, which were calibrated with a KI-linked HRP assay at pH 5.4 (ε at 353 nm = 25 500 mM⁻¹ cm⁻¹; Cotton & Dunford, 1973). Continuous assay of H₂O₂ formation in K329A reactions was not possible due to instability of the oxidized ABTS chromophore at pH 8 and the low rate of H₂O₂ production by K329A. Instead, the amount of H₂O₂ accumulated in quenched reactions was quantified relative to side-product concentrations determined in parallel by anion-exchange analysis. A reaction containing catalase was included as a control. Because of the potential to degrade H₂O₂ and interfere with ABTS, 2-mercaptoethanol was removed from Rubisco stocks by exhaustive dialysis at 4 °C versus thiol-free buffer. Exclusion of 2-mercaptoethanol did not affect the distribution of RuBP-derived products observed in chromatographic product analyses (data not shown).

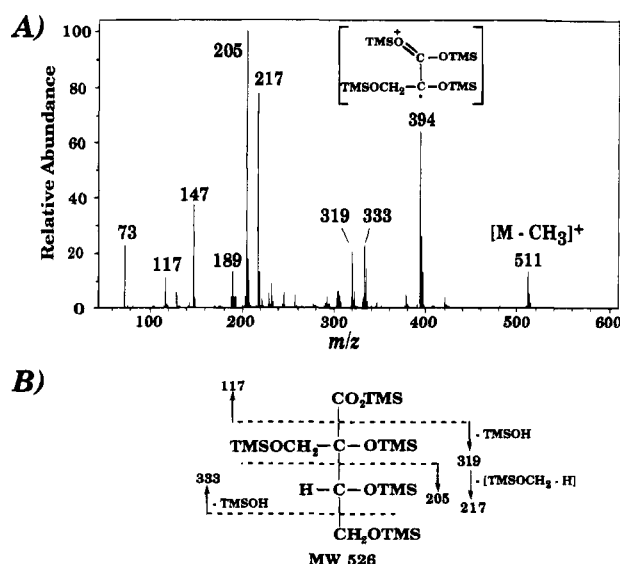


FIGURE 2: (A) Electron-impact mass spectrum obtained by GC-MS of TMS-derivatized dephosphorylated CTBP. The ion depicted at *m/z* 394 corresponds to a McLafferty-rearrangement fragment formed from TMS migration to the carboxyl carbonyl. (B) Proposed fragmentation pattern.

Reactions for H₂O₂ analyses contained 50 mM bicine, 10 mM MgCl₂, 1 mM EDTA, 10.5 mM NaHCO₃, 10% (v/v) glycerol, 1.1 mg/mL K329A, ± 1000 units/mL catalase, and 200 μM [1-³H]RuBP (2.3 × 10⁶ cpm/μmol) at pH 8. At the indicated times, duplicate aliquots were quenched with an equal volume of 2 M sodium acetate (pH 5.4) for H₂O₂ determination or 1% (w/v) SDS for anion-exchange analysis. The acidified samples were cooled on ice, and after centrifugation the supernatants were analyzed immediately. The HRP-linked spectrophotometric assay (500 μL) contained 175–275 mM sodium acetate (pH 5.4), 0.5 mM ABTS, and 50 units/mL HRP. H₂O₂ was determined from the increase in absorbancy at 414 nm observed after addition of an aliquot (50–100 μL) of the acidified K329A reaction. The maximal reading, obtained immediately, was stable for several seconds. SDS-quenched reaction aliquots were diluted with water and deproteinized prior to analysis by anion-exchange chromatography. Concentrations of RuBP-derived side products were estimated from the percentage of total radioactivity contained in the respective chromatographic peaks.

RESULTS

Structural Analyses. Proof of structure of compound X as CTBP was provided by MS, NMR, and chemical degradation. GC-MS analysis of the TMS derivative of the alkaline phosphatase-treated unknown revealed an [M - 15]⁺ ion at *m/z* 511 due to loss of a methyl radical from the unobserved molecular ion at *m/z* 526 (Figure 2A). The ions at *m/z* 394, due to McLafferty rearrangement involving TMS-migration (Pettersson, 1992), and *m/z* 117, due to [COOTMS]⁺, establish the presence of a carboxyl substituent. In combination with results obtained with CTBP derived from [2-¹³C]RuBP (see below), the observed spectrum fits the expected fragmentation of penta-TMS derivatized 2-carboxytetritol (Figure 2B). A base ion ([M - H]⁻) at *m/z* 165 was observed during ESI-MS analysis of the underivatized dephosphorylated unknown (Figure 1 in the supporting

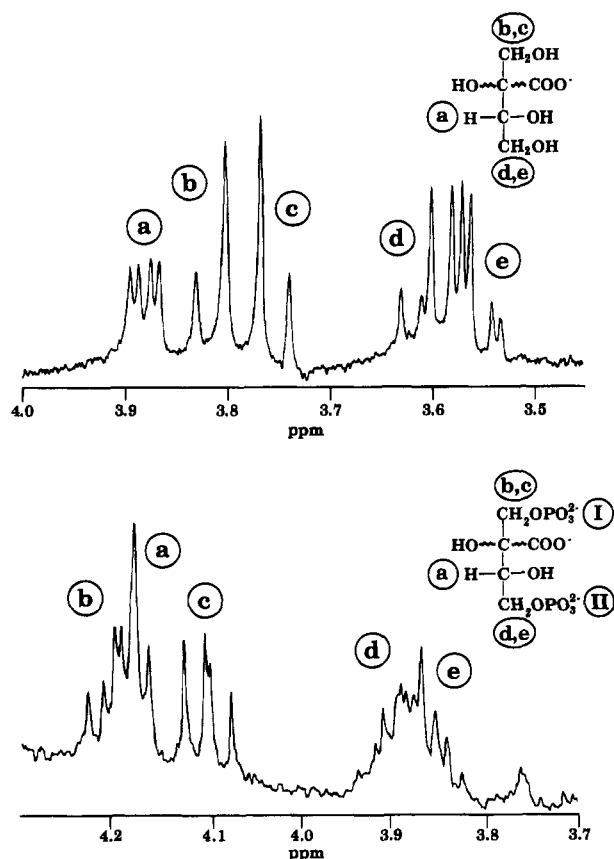


FIGURE 3: ^1H NMR spectra of dephosphorylated CTBP (top) and CTBP (bottom). Spectral acquisition conditions are given in Experimental Procedures. The wavy bonds around C2 denote uncertainty about absolute stereoconfiguration.

Table 1: Coupling Constants Measured for CTBP Nuclear Interactions

	coupling constant (Hz)	
	phosphatase-treated CTBP	CTBP
$J_{\text{Ha-Hc}}$	3.5	5.5
$J_{\text{Ha-Hd}}$	8.2	7.0
$J_{\text{Hd-Hc}}$	12.1	11.0
$J_{\text{Hb-Hc}}$	11.3	11.5
$J_{\text{Hb-PI}}$		7.0
$J_{\text{Hc-PI}}$		9.4
$J_{\text{Hd-PII}}$		6.7
$J_{\text{He-PII}}$		5.8
$J_{\text{C1-C2}}$	NA ^a	42.9
$J_{\text{C2-C3}}$	NA	41.9
$J_{\text{C3-C4}}$	NA	42.9
$J_{\text{C2-COO}^-}$	NA	55.4

^a Not available.

information). The empirical formula for this ion, $\text{C}_5\text{H}_9\text{O}_6$, fits a carboxyl-containing 5-carbon polyol.

The ^1H NMR spectrum obtained for the dephosphorylated unknown shows three clusters of resonances integrating in a ratio of 1:2:2 (Figure 3, top). The chemical shifts, splitting patterns, and magnitudes of coupling constants (Table 1) correlate with the presence of one vicinally coupled proton (H_a) and two pairs of geminal protons; one of the latter pairs is isolated (H_b/H_c) and the other (H_d/H_e) is coupled to H_a . Assignments were verified by selective decoupling, COSY (data not shown) and TOCSY (Figure 2 in supporting information) experiments. The absence of coupling between the H_b/H_c pair and any of the other three protons (even with

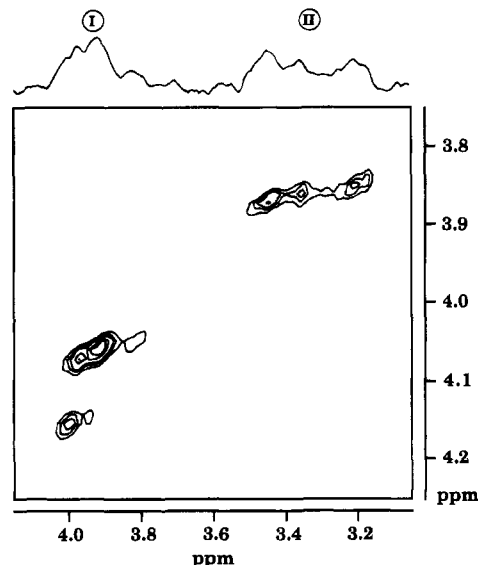


FIGURE 4: ^1H - ^{31}P COLOC spectrum of CTBP. The ^{31}P signals (F_2 dimension) are projected onto the upper horizontal axis. The vertical scale (F_1 dimension) corresponds to the ^1H dimension (see Figure 3, bottom). Resonance designations (I, II) refer to the assignments made in the structure inset in Figure 3, bottom. Spectral acquisition conditions are given in Experimental Procedures.

mixing times >50 ms) denotes a break in proton-proton connectivity within the molecule. The ^1H NMR spectrum for the parent (phosphorylated) compound contains three clusters of signals also integrating as five protons in a ratio of 2:1:2 (Figure 3, bottom). Although this spectrum is further complicated by additional scalar couplings from phosphorus substituents, TOCSY analysis (Figure 3 in supporting information) revealed proton-proton coupling between the most downfield cluster (H_b , H_c) and both the central (H_d) and most upfield (H_a , H_e) clusters, but not between the latter two groups. As in the case of the dephosphorylated compound, these results imply two groups of noninteracting protons.

Broad-band decoupling (data not shown) and COLOC (Figure 4) experiments with X indicate that all protons except H_a are coupled to phosphorus. The two equal-intensity phosphorus resonances in the ^{31}P NMR spectrum (shown in the F_2 dimension of Figure 4) reflect the presence of two phosphorus-containing substituents in the parent compound. Each phosphorus couples to one of the pairs of methylene protons with H-P coupling constants (5.8–7 Hz) in the range for three-bond coupling (Table 1), as required by a structure containing two terminal phosphate-substituted methylene groups.

The connectivity of carbon atoms in CTBP was deduced by ^{13}C NMR of the compound generated from [U - ^{13}C]RuBP (Figure 5A). The presence of five carbon resonances shows conservation of all carbons of RuBP. The carbon-carbon coupling pattern (Table 1) fits a branched backbone, with the resonance for the branching carbon shifting in the carbonyl region. Qualitatively, the smaller intensities of the resonances at 178 and 77 ppm are indicative of nonprotic carbons. On the basis of chemical shift, the MS results, and the observation that the molecule retains a net -1 charge after phosphatase treatment (Harpel & Hartman, 1994), the branching carbon is assigned as a carboxylate.

Two additional NMR experiments confirm the assignments of ^1H and ^{13}C resonances. The first, an INEPT experiment, utilized proton-to-carbon magnetization transfer to visualize

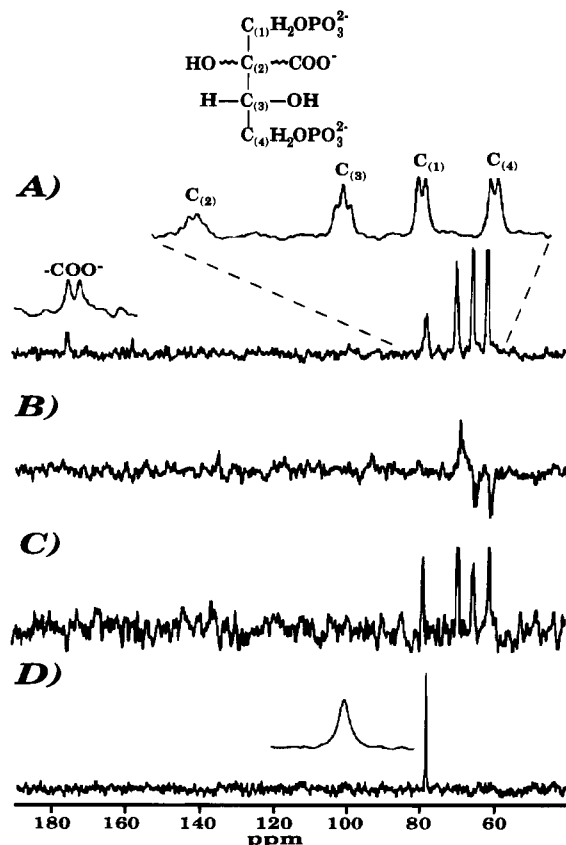


FIGURE 5: ^{13}C NMR spectroscopy (^1H -decoupled) of ^{13}C -enriched CTBP. (A) Spectrum of $[U\text{-}^{13}\text{C}]$ CTBP derived from $[U\text{-}^{13}\text{C}]$ RuBP, with enlargements emphasizing the ^{13}C - ^{13}C splitting patterns. (B) INEPT spectrum of $[U\text{-}^{13}\text{C}]$ CTBP. (C) Carbon-carbon relayed INEPT spectrum of $[U\text{-}^{13}\text{C}]$ CTBP. (D) Spectrum of $[2\text{-}^{13}\text{C}]$ CTBP derived from $[2\text{-}^{13}\text{C}]$ RuBP. The wavy bonds around C2 denote the uncertain absolute stereoconfiguration. Spectral acquisition conditions: (A and D) 32K data points, 1 s relaxation delay, 0.524 s acquisition time, 256 scans, 20 Hz line broadening; (B) 16K data points, 3 s relaxation delay, 512 scans, 40 Hz line broadening, 2.2 ms delay; (C) same as for B, but with 1024 scans, 2.2 ms delay (for XH coupling), and 5 ms delay (for XX coupling).

only those carbons with protons directly attached. The resulting spectrum (Figure 5B) contains two resonances due to $-\text{CH}_2-$ substitution (negative peaks) and one due to $-\text{CH}$ - (or $-\text{CH}_3$; positive peak); from the couplings observed in Figure 5A, the latter carbon is coupled to one of the former. The absence of the two lower-intensity peaks observed in Figure 5A verifies that neither carbon contains proton substituents. The second experiment was a carbon-carbon relayed INEPT sequence, in which magnetization transferred from protons to directly attached carbons was then relayed to adjacent carbons via carbon-carbon coupling. The absence of the resonance for the carbonyl carbon (Figure 5C) shows that its only neighbor is a nonprotic carbon. Combining these results with the observed carbon-carbon couplings (Table 1), the resonance at 77 ppm must therefore be a quaternary carbon connecting the two sets of proton-substituted carbon centers. The two $-\text{CH}_2-$ carbons were assigned on the basis of coupling to protons by a heteronuclear COSY experiment (data not shown).

As a whole, the NMR data best support the structure $\text{C}(\text{H}_2\text{OPO}_3^{2-})\text{-C}(?, \text{COO}^-)\text{-C}(?, \text{H})\text{-C}(\text{H}_2\text{OPO}_3^{2-})$. From the MS data, the two unidentified substituents ("?) must be hydroxyl groups, identifying the compound as 2-carboxytetritol 1,4-bisphosphate (CTBP). Our data do not identify the stereo-

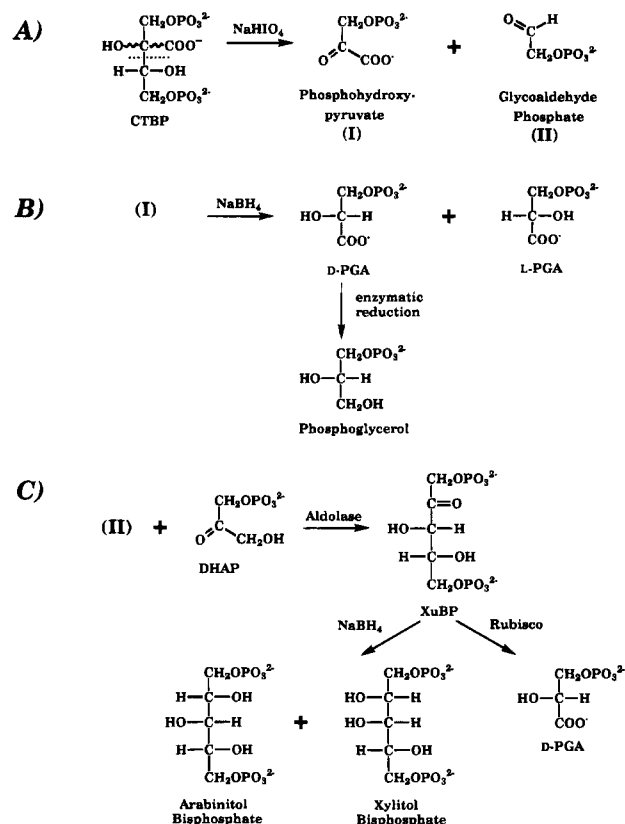


FIGURE 6: Scheme for chemical characterization of CTBP by periodate oxidation and identification of cleavage products. Phosphohydroxypyruvate (I) is observed from oxidation of CTBP derived from $[1\text{-}^3\text{H}]$ RuBP. Glycoaldehyde phosphate (II) is observed from oxidation of CTBP derived from $[5\text{-}^3\text{H}]$ RuBP.

chemical configuration of C2 of CTBP; C3 is assumed to maintain the D configuration of C4 of RuBP, from which it is derived (see Discussion).

The fate of individual carbon atoms from RuBP during formation of CTBP was probed using material derived from turnover of $[2\text{-}^{13}\text{C}]$ RuBP by K329A. By NMR, ^{13}C enrichment was found only at the position assigned to the quaternary carbon (Figure 5D). GC-MS also supports this assignment, with ions observed for the individually ^{13}C -enriched dephosphorylated compound at m/z 512, 395, 320, 218, 205, and 117 (data not shown). The single mass-unit increase in fragments no longer containing the carboxyl group (e.g., 320 and 218; see Figure 2B) locates the ^{13}C label within the CTBP backbone; the ions at 205 and 117 were unenriched. These results limit the plausible mechanisms for formation of CTBP by K329A.

Chemical Degradation by Sodium Periodate. The assignments of nonprotic substituents, two terminally disposed phosphate esters, and a quaternary carbon connecting the two phosphate-containing segments of CTBP were verified by periodate oxidation of material derived from $1\text{-}^3\text{H}$ - and $5\text{-}^3\text{H}$ -labeled RuBP. Relatively rigorous conditions (15-fold molar excess periodate for 7.5 h at room temperature) were required to oxidatively cleave CTBP, as expected for a compound with an α -carboxy substituent at the cleavage site (Pigman & Goep, 1948).

The oxidation products derived from CTBP are those predicted for the assigned structure (Figures 6 and 7). The primary labeled product derived from $[1\text{-}^3\text{H}]$ CTBP was identified as phosphohydroxypyruvate by successive chemi-

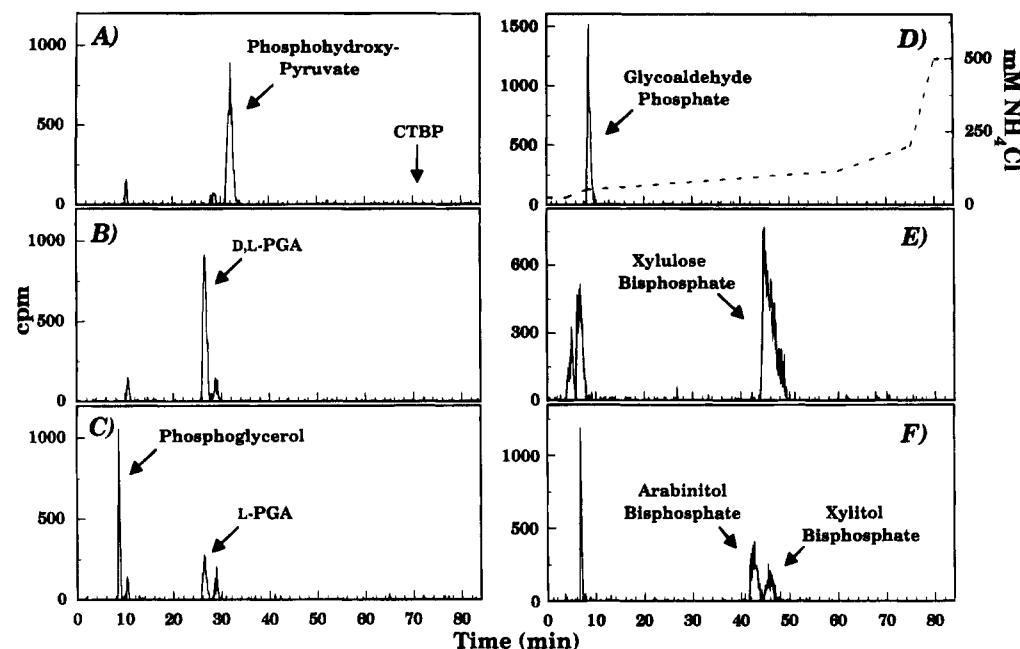


FIGURE 7: Anion-exchange analysis of periodate cleavage products and derivatives from $[1\text{-}^3\text{H}]\text{CTBP}$ (left column; derived from $[1\text{-}^3\text{H}]\text{RuBP}$) and $[4\text{-}^3\text{H}]\text{CTBP}$ (right column; derived from $[5\text{-}^3\text{H}]\text{RuBP}$). (A and D) Initial periodate oxidation products. Identification of phosphohydroxypyruvate (I) was via (B) borohydride reduction to yield racemic PGA and (C) further enzymatic reduction specific for D-PGA. Identification of glycoaldehyde phosphate (II) was via aldol condensation with dihydroxyacetone phosphate to yield XuBP (E), which was further identified by borohydride reduction (F) and by turnover by wild-type Rubisco (data not shown). The elution gradient depicted in panel D by the dashed line was used throughout.

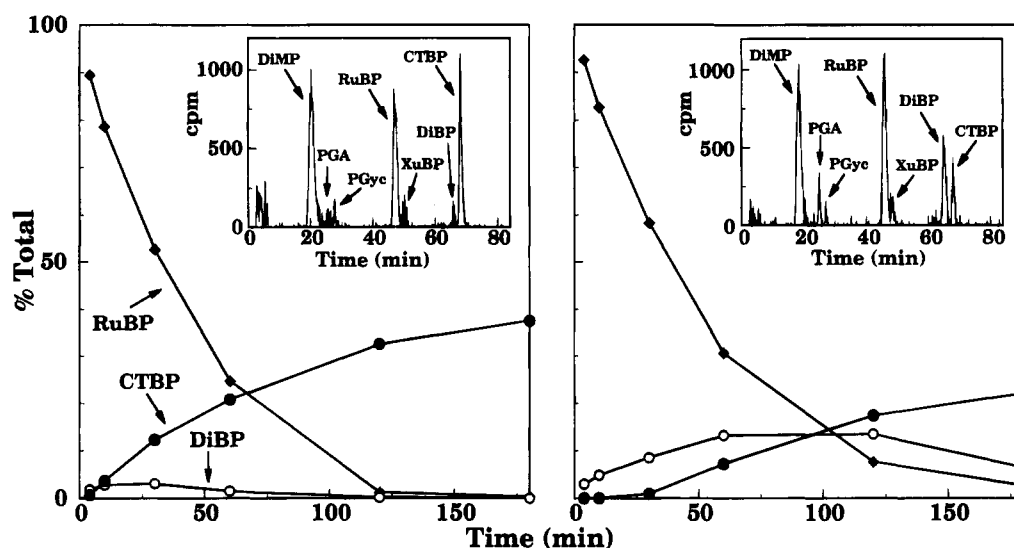


FIGURE 8: Time courses for $[1\text{-}^3\text{H}]\text{RuBP}$ turnover by K329A in the absence (left) and presence (right) of 50 sodium borate. Inset profiles are 60 min time points.

cal and enzymatic reduction to form D,L-PGA and phosphoglycerol, respectively. The primary labeled product derived from $[4\text{-}^3\text{H}]\text{CTBP}$ was identified as glycoaldehyde phosphate by aldolase-coupled condensation with DHAP to form XuBP, which was characterized by chemical reduction and by turnover by wild-type Rubisco. Most importantly, C2 was identified as a carboxyl- and hydroxyl-substituted quaternary carbon. The small peak eluting at ~ 28 min in the profiles for material obtained from $[1\text{-}^3\text{H}]\text{CTBP}$ is due to a small amount of PGyc, which resulted from slight periodate cleavage of phosphohydroxypyruvate.

A structurally related compound, $[^{14}\text{C}\text{-carboxy}]\text{CABP}$, was also subjected to periodate oxidation. Formation of $[^{14}\text{C}\text{-carboxy}]\text{phosphohydroxypyruvate}$ as the primary radiola-

beled product verifies that CTBP and CABP share the same substituents at carbons 1 and 2 (data not shown).

Formation of CTBP. Time courses for K329A reactions with $[1\text{-}^3\text{H}]\text{RuBP}$ were analyzed in order to gain insight into the origin of CTBP. A transient species (denoted as "DiBP" in Figure 8) was observed in intermediate-time profiles, in addition to the previously noted (Harpel & Hartman, 1994) stable end products: CTBP, PGA (from trace carboxylation activity), PGyc (from trace oxygenase activity), and the dicarbonyl monophosphate 1-deoxy-D-glycero-2,3-pentodiulose 5-phosphate (denoted "DiMP" in Figure 8; from β -elimination of phosphate from the enediol intermediate).³ The transient, although initially thought to be 3-ketoarabinol 1,5-bisphosphate (Harpel & Hartman, 1994; Lee et al., 1993),

Table 2: H₂O₂ and Side Product Formation by K329A

reaction	time (h)	% conversion ^a	[H ₂ O ₂] ^b (μM)	[CTBP] ^c (μM)	[dicarbonyl bisphosphate] ^c (μM)	[total] ^d (μM)	[H ₂ O ₂]/[total]
(A) K329A + RuBP	1	80	34	42	4	46	0.74
	3	97	28	54	0	54	0.52
(B) K329A + catalase + RuBP	1	85	0	55	4	59	0
	3	97	0	66	0	66	0

^a 100 minus the combined percentage of total counts collected that represent RuBP and XuBP. ^b Determined by ABTS/HRP reaction; all values are corrected for the contribution (3 μM) due to background absorbancy in all samples. ^c Determined by anion exchange chromatography on Mono Q. ^d [CTBP] + [dicarbonyl bisphosphate].

has been identified as D-glycero-2,3-pentodiulose 1,5-bisphosphate (Chen & Hartman, 1995). An apparent burst in the appearance of this dicarbonyl bisphosphate prior to accumulation of CTBP (Figure 8, left) argues for a precursor-product relationship. An initial lag and slower overall rate in CTBP production, which coincides with trapping of the dicarbonyl bisphosphate species by borate (Figure 8, right), also supports this relationship.

A small amount of XuBP (Figure 8, insets) is formed from misprotonation at C3 of the enediol intermediate (Edmondson et al., 1990). Although XuBP is also a transient and an alternate substrate for K329A, it was converted to the full spectrum of RuBP-derived K329A reaction products (data not shown). Therefore, XuBP is not an immediate precursor to CTBP. The material eluting near the solvent front primarily reflects trace phosphatase contamination in the K329A preparation.

Identification of an oxidized form of RuBP, the dicarbonyl bisphosphate, as a precursor to CTBP suggested that a reduced oxygen species might also be formed during RuBP turnover by K329A. Proof was obtained in peroxidase-linked assays for H₂O₂ accumulation in reactions of K329A (Table 2). H₂O₂ was not evident above background levels for reactions quenched immediately upon initiation with RuBP. However, samples quenched after 1 h contained H₂O₂ at levels approaching the concentrations of dicarbonyl bisphosphate and CTBP. The ratio of ~0.7 between H₂O₂ and the combined concentrations of the two side products likely reflects a 1:1 stoichiometry, given the instability of H₂O₂ in the reaction (note the reduced peroxide/product ratio after 3 h); a control reaction, lacking RuBP but spiked with 100 μM H₂O₂, showed ~20% loss of H₂O₂ over 1 h. The lack of H₂O₂ accumulation in the catalase-containing control provides proof of H₂O₂ specificity in the HRP assay. Similarly, H₂O₂ was not found in reactions containing RuBP and lacking K329A or in wild-type Rubisco reactions (data not shown).

Dicarbonyl Bisphosphate as an Alternate Substrate for K329A. The precursor-product relationship between dicarbonyl bisphosphate and CTBP was independently tested by evaluating the ability of K329A to utilize the dicarbonyl bisphosphate as a substrate. K329A converted isolated

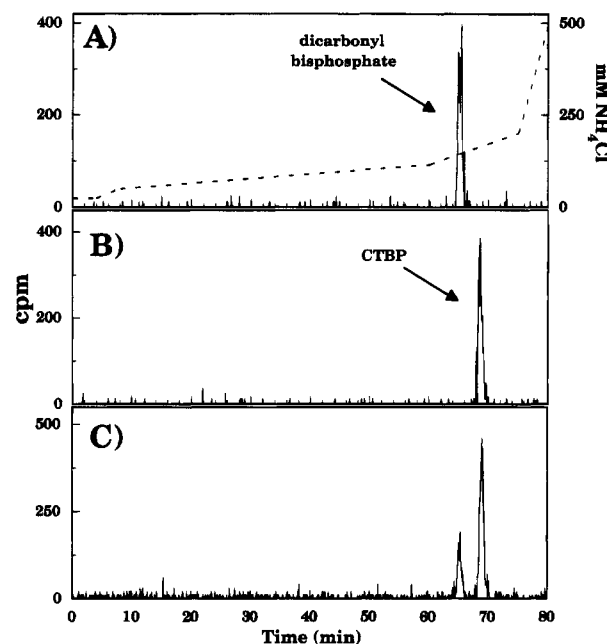


FIGURE 9: Turnover of isolated 1-³H-labeled D-glycero-2,3-pentodiulose 1,5-bisphosphate by K329A. Starting material (A), the K329A reaction mixture (B), and a mixture of authentic 1-³H-labeled dicarbonyl bisphosphate and [4-³H]CTBP (C) were chromatographed on Mono Q, as described in the text. The K329A reaction mixture contained 0.4 mg/mL K329A, 150 mM bicine (pH 8), 20 mM NaHCO₃, 255 μM O₂, 10 mM MgCl₂, 1 mM EDTA, and 2.4 μM 1-³H-labeled dicarbonyl bisphosphate. The reactions also contained 7 mM sodium borate and 130 mM NaCl carried over from purification of the dicarbonyl bisphosphate. After incubation for 4 h at 23 °C, the reaction was quenched with 1% (w/v) SDS and 1 mM NaBH₄. Any unprocessed dicarbonyl bisphosphate would be reduced to a mixture of pentitol bisphosphates, which would elute from ~40–50 min (Chen & Hartman, 1995). After 15 min, excess NaBH₄ was consumed with 2.2 mM glucose.

dicarbonyl bisphosphate (obtained from reactions of the E48Q mutant of Rubisco; Chen & Hartman, 1995) completely and exclusively to CTBP (Figure 9). The conversion of dicarbonyl bisphosphate is independent of O₂ (data not shown), as demonstrated by production of CTBP in the presence of an O₂-scrubbing system (Harpel et al., 1993). No CTBP was formed in reactions lacking the enzyme.

DISCUSSION

Recognizing that aberrant products generated by Rubisco mutants can provide mechanistic insights [reviewed in Hartman and Harpel (1993, 1994), Andrews et al. (1994), and Harpel et al. (1995)], we have pursued the structural identification and genesis of a novel O₂-dependent side product, compound X, formed during the turnover of RuBP by the K329A mutant (Harpel & Hartman, 1994). Our

³ CTBP (via DiBP), PGyc, PGA, DiMP, and XuBP represent alternate partitioning of the enediol intermediate through oxygenation, carboxylation, β-elimination, and misprotonation pathways, respectively. Based on the average molar ratio of the product of β-elimination (DiMP) versus the combined products of "successful" forward processing (CTBP + DiBP + PGA + PGyc) under the experimental conditions of Figure 7, the apparent partition ratio approximates 1.3:1 in favor of elimination. This value should not be considered a true partition coefficient, because of our lack of knowledge concerning potential reversibility of peroxyketone formation.

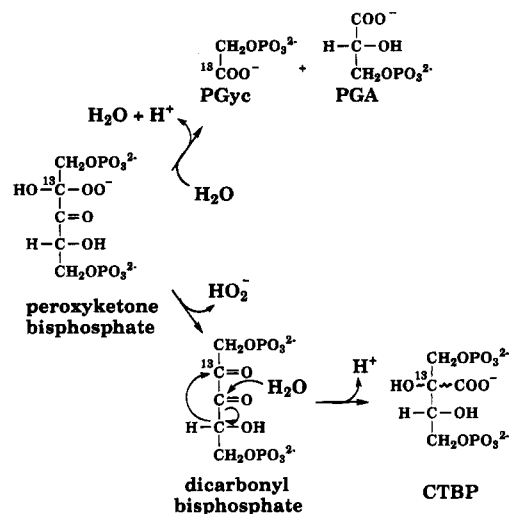


FIGURE 10: Oxygenase reactions catalyzed by Rubisco. The upper branch from the peroxy intermediate represents formation of the products of wild-type oxygenase activity. The lower branch is proposed for the formation of the dicarbonyl bisphosphate and CTBP by K329A. The superscript "13" traces the fate of C2 of RuBP through the two pathways.

results identify X as CTBP and suggest a pathway for its formation (Figure 10). Corroborative evidence for the pathway depicted includes the production of H_2O_2 and identification of the dicarbonyl, D-glycero-2,3-pentodiulose 1,5-bisphosphate, as the immediate precursor. Retention of all five carbon atoms of RuBP in a branched-chain carboxy-substituted structure necessarily invokes a rearrangement mechanism stemming from an oxygenase-related intermediate derived from the enediol of RuBP.

A C2-peroxy adduct of the RuBP enediol, resulting from recombination of a superoxide-enediol radical caged pair (Lorimer, 1981), has been proposed as Rubisco's oxygenation intermediate on the basis of the ^{18}O -labeling pattern of the oxygenase products (Lorimer et al., 1973). To date, the only physical evidence for this intermediate has been $^{17}\text{O}_2$ -dependent hyperfine interactions observed in the EPR spectrum of Cu^{2+} -replaced Rubisco (Brändén et al., 1984). Because only elimination of H_2O_2 from a peroxy adduct of the enediol can account for oxidation of the RuBP enediol to generate the dicarbonyl bisphosphate precursor to CTBP, formation of the dicarbonyl bisphosphate and CTBP thus provide direct proof for the proposed peroxyketone intermediate in Mg^{2+} -activated Rubisco. These two novel O_2 -dependent side products also provide new indicators for evaluating the integrity of oxygenation activity of Rubisco mutants.

By analogy to peroxy intermediates of flavin-containing oxidases [reviewed in Massey (1994)], several fates can be envisioned for an α -keto peroxide generated by Rubisco: forward processing (hydrolytic C—C cleavage), elimination of peroxide (heterolytic C—O cleavage), formation of superoxide anion plus a carbon-based radical (homolytic C—O cleavage), and reversal of O_2 addition. Because the flavin hydroperoxide is unstable in aqueous solutions, differential stabilization of the transition state for the flavin- O_2 addition step dictates the type of reaction catalyzed by each flavin-dependent oxidase; only with flavin hydroxylases, which catalyze oxygen-insertion reactions, has a stable flavin hydroperoxide intermediate been proven (Massey, 1994).

Rubisco's peroxy intermediate should be similarly unstable. Our results indicate that Rubisco must properly stabilize the peroxy intermediate for efficient cleavage of the C2—C3 and peroxy O—O bonds and thereby avoid pathways other than production of PGA and PGyc as predominates with wild-type Rubisco. Of the potential fates for this intermediate, only forward processing, to a very minor extent in forming PGA and PGyc, and heterolytic cleavage, to a much greater extent in forming dicarbonyl bisphosphate, occur with K329A. Reversibility of Rubisco's peroxy intermediate has not been addressed directly, but the corresponding carboxylated reaction intermediate (A in Figure 1) is fully committed to forward processing with both wild-type Rubisco (Pierce et al., 1986) and position-329 mutants (Lorimer et al., 1993). Chemiluminescence associated with Mn^{2+} -replaced Rubisco (Mogel & McFadden, 1990) may reflect reversal of the peroxy intermediate to singlet oxygen, although the source of chemiluminescence has been disputed (Lilley et al., 1993). Homolytic cleavage of the O—O bond does not appear to be a significant event with K329A.⁴

Our data do not clearly distinguish between formation of dicarbonyl bisphosphate within the K329A active site or formation in solution subsequent to release of the peroxy intermediate due to destabilization of the closed conformation of loop 6. However, the rearrangement to CTBP is catalyzed by K329A, as shown by the K329A-dependent conversion of isolated dicarbonyl bisphosphate to CTBP; the dicarbonyl bisphosphate does not undergo spontaneous rearrangement under the weakly alkaline conditions of our assay (pH 8).

Rearrangement of the dicarbonyl bisphosphate precursor to form CTBP is preceded by base-catalyzed rearrangements of aliphatic α -dicarbonyls to α -hydroxy acids and by similar anionic rearrangement mechanisms [reviewed in Selman and Eastham (1960)]. The most thoroughly studied of these is the benzylic acid rearrangement, which involves hydroxide-initiated 1,2-aryl migration within a vicinal diketone (Geissman, 1960; Cram, 1965). An even closer analogy to the formation of CTBP is provided by the base-catalyzed rearrangement of 1-deoxy-D-glycero-2,3-pentodiulose 5-phosphate (derived from β -elimination of phosphate from RuBP) to methyl tetronic acid 4-phosphate (Paech et al., 1978).

The course of the dicarbonyl rearrangement for CTBP formation follows principles similar to those of the model reactions, as revealed by the fate of ^{13}C label derived from $[2-^{13}\text{C}]\text{RuBP}$ (Figure 10). Enrichment of only the quaternary carbon of CTBP requires that migration occurs by a 1,2-shift following hydration at C3 of the dicarbonyl. Thus, migratory aptitude is governed by the electron-releasing potential of the C4 atom and the electron-withdrawing properties of the carbonyl at C2, which is situated β to a phosphate group. K329A presumably initiates the rearrangement reaction through an inherent activity of the enzyme, i.e., C3-carbonyl hydration. As position-329 mutants are also competent in the forward processing of isolated carboxyketone intermediate (Lorimer et al., 1993), we conclude that

⁴ We have assayed for superoxide and carbon-based radicals with cytochrome *c* and radical-trapping agents, respectively. Neither significant reduction of cytochrome *c* nor alteration of product distributions by various radical scavengers, indicative of stable adduct formation, was observed. These negative results do not rigorously exclude formation of the radical side products but, in combination with our other observations, suggest that these are not major species.

Lys329 is not essential for hydration at C3 in either the carboxylation or oxygenation pathway. Formation of dicarbonyl biphosphate may then not represent inability of the enzyme to hydrolytically cleave the peroxy intermediate, per se, but inability to stabilize it within the active site. A priori, rearrangement of the dicarbonyl biphosphate within Rubisco's active site is tenable, given the active-site flexibility required in later stages of the carboxylation reaction (Larimer et al., 1994; Morrell et al., 1994).

Although the dicarbonyl biphosphate (but not CTBP) and H_2O_2 are also formed from RuBP by a site-directed mutant substituted at the neighboring residue, Glu48 (Chen & Hartman, 1995), unique oxygenase products other than PGyc have yet to be observed with wild-type *R. rubrum* Rubisco. This may be taken as a further indication of active stabilization of the peroxy intermediate by Rubisco, despite the negative impact of the oxygenation reaction on photosynthetic efficiency. If oxygenation of RuBP is an unavoidable consequence of the reactivity of the enediol intermediate (Lorimer & Andrews, 1973), formation of PGA and PGyc would be a more favorable outcome than formation of the dicarbonyl biphosphate and CTBP. The PGA can be used for carbon assimilation, and some of the carbon lost to PGyc can be recovered through the glycolate pathway [reviewed in Andrews and Lorimer (1987) and Ogren (1984)], although at a cost of energy. The dicarbonyl biphosphate and CTBP, in contrast, would likely be dead-end products for photosynthetic organisms.

Our present results implicate Lys329 in the stabilization of the peroxy intermediate in addition to the roles previously attributed to this residue in activating the enediol for attack by CO_2 and in stabilizing the carboxylation intermediate [summarized in Harpel et al. (1995)]. In the absence of structural data, the precise interactions between the peroxy intermediate and Lys329 are subject to speculation. However, the impairment of K329A in stabilizing both the peroxyketone and carboxyketone intermediates may suggest similar transition states and similar active-site interactions for the two reactions. The ϵ -amine of Lys329 could stabilize a peroxide oxyanion through ionic interaction, in analogy to the amine/carboxylate-oxyanion interaction visualized in the 3D structure of the enzyme complexed with CABP, or by hydrogen-bonding to a Mg^{2+} -coordinated peroxy group. By stabilizing the closed conformations of flexible loop 6 and the flexible N-terminal segment of the active site through the intersubunit salt bridge with Glu48, Lys329 would help protect this labile intermediate by sequestration from solvent. Lys329 must also play an active role in promoting addition of O_2 , as well as CO_2 , to the enediol of RuBP; despite the accumulation of the O_2 -related side products, the rate of appearance of these products is small relative to the k_{cat} for wild-type oxygenase activity. Catalytic assistance in O_2 addition may be a consequence of promoting geometric deformation of the enediol, which has been proposed in theoretical studies to activate this intermediate for attack by CO_2 and/or O_2 (Andrés et al., 1992, 1993; Tapia et al., 1992).

In conclusion, we propose that the basic tenets of our study are applicable to other oxygenases that rely solely on substrate-derived carbanions for O_2 reactivity. To catalyze oxygenation, these enzymes, like Rubisco, must also activate a carbanion for electrophilic attack by O_2 by stabilizing both the O_2 addition transition state and reaction intermediates beyond the point of addition. Subtleties of these mechanisms

may vary among the enzymes. For example, the metal ion in acetolactate synthase II does not appear to play a direct role in oxygenation (Tse & Schloss, 1993), whereas the metal is clearly involved in promoting oxygenation by Rubisco (Schloss, 1990; Robison et al., 1979; Christeller & Laing, 1979). However, principles governing productive oxygenation are generally applicable. In analogy with the K329A mutant, glutamate decarboxylase eliminates H_2O_2 from a peroxy intermediate ["unpublished observation" in Tse and Schloss (1993)]. Hydroxypyruvaldehyde phosphate and PGA both accompany oxygen consumption by class II aldolase. The former compound, a dicarbonyl, derives from heterolytic cleavage and elimination of H_2O_2 from a peroxy adduct of DHAP (Abell & Schloss, 1991); the latter product could represent hydration of the dicarbonyl and 1,2-hydride transfer. Chemiluminescence similar to that attributed to Rubisco's oxygenation reaction (Mogel & McFadden, 1990) has also been reported for the Mn^{2+} -replaced forms of acetolactate synthase (Tse & Schloss, 1994; Durner et al., 1994). Further comparisons between Rubisco and these enzymes await more complete characterization of the latter's side reactions.

ACKNOWLEDGMENT

We are indebted to our colleague Dr. Y.-R. Chen for providing the isolated dicarbonyl biphosphate and assisting with associated turnover studies. We thank Professors J. V. Schloss (University of Kansas) and R. D. Libby (Moravian University) for advice on assays for H_2O_2 , Ms. C. G. Shibata and Dr. J. D. Gregory (University of Tennessee) for preliminary NMR data, and Drs. S. A. McLuckey and S. Habibi-Goudarzi (Chemical and Analytical Sciences Division, ORNL) for obtaining ESI-MS data.

SUPPORTING INFORMATION AVAILABLE

Three figures showing the ESI-MS profile and TOCSY spectrum of dephosphorylated CTBP (3 pages). Ordering information is given on any current masthead page.

REFERENCES

- Abell, L. M., & Schloss, J. V. (1991) *Biochemistry* 30, 7883–7887.
- Andersson, I., Knight, S., Schneider, G., Lindqvist, Y., Lundqvist, T., Brändén, C.-I., & Lorimer, G. H. (1989) *Nature* 337, 229–234.
- Andrés, J., Safont, V. S., & Tapia, O. (1992) *Chem. Phys. Lett.* 198, 515–520.
- Andrés, J., Safont, V. S., Queralto, J., & Tapia, O. (1993) *J. Phys. Chem.* 97, 7888–7893.
- Andrews, T. J., & Lorimer, G. H. (1987) in *The Biochemistry of Plants* (Hatch, M. D., & Boardman, N. K., Eds.) Vol. 10, pp 131–218, Academic Press, New York.
- Andrews, T. J., Morell, M. K., Kane, H. J., Paul, K., Quinlan, G. A., & Edmondson, D. L. (1994) in *Carbon Dioxide Fixation and Reduction in Biological and Model Systems* (Brändén, C.-I., & Schneider, G., Eds.) pp. 53–68, Oxford University Press, Oxford.
- Bowes, G., Ogren, W. L., & Hageman, R. H. (1971) *Biochem. Biophys. Res. Commun.* 45, 716–722.
- Brändén, R., Nilsson, T., & Styring, S. (1984) *Biochemistry* 23, 4378–4382.
- Chen, Y.-R., & Hartman, F. C. (1995) *J. Biol. Chem.* 270, 11741–11744.
- Childs, R. E., & Bardsley, W. G. (1975) *Biochem. J.* 145, 93–103.

- Christeller, J. T., & Laing, W. A. (1979) *Biochem. J.* 183, 747–750.
- Cotton, M. L., & Dunford, H. B. (1973) *Can. J. Chem.* 51, 582–587.
- Cram, D. J. (1965) *Fundamentals of Carbanion Chemistry*, pp 239–243, Academic Press, New York.
- Durner, J., Gailus, V., & Böger, P. (1994) *FEBS Lett.* 354, 71–73.
- Edmondson, D. L., Kane, H. J., & Andrews, T. J. (1990) *FEBS Lett.* 260, 62–66.
- Geissman, T. A. (1960) *Principles of Organic Chemistry*, pp 678–680, W. H. Freeman and Company, San Francisco.
- Gutteridge, S., Rhoades, D. F., & Herrmann, C. (1993) *J. Biol. Chem.* 268, 7818–7824.
- Hamilton, G. A. (1974) in *Molecular Mechanisms of Oxygen Activation* (Hayaishi, O., Ed.) pp 405–451, Academic Press, New York.
- Harpel, M. R., & Hartman, F. C. (1994) *Biochemistry* 33, 5553–5561.
- Harpel, M. R., Larimer, F. W., & Hartman, F. C. (1991) *J. Biol. Chem.* 266, 24734–24740.
- Harpel, M. R., Lee, E. H., & Hartman, F. C. (1993) *Anal. Biochem.* 209, 367–374.
- Harpel, M. R., Serpersu, E. H., & Hartman, F. C. (1995) in *Techniques in Protein Chemistry VI*, (Crabb, J. W., Ed.) pp 357–364, Academic Press, San Diego.
- Hartman, F. C. (1971) *Biochemistry* 10, 146–154.
- Hartman, F. C., & Lee, E. H. (1989) *J. Biol. Chem.* 264, 11784–11789.
- Hartman, F. C., & Harpel, M. R. (1993) *Adv. Enzymol. Relat. Areas Mol. Biol.* 67, 1–75.
- Hartman, F. C., & Harpel, M. R. (1994) *Annu. Rev. Biochem.* 63, 197–234.
- Horecker, B. L., Hurwitz, J., & Weissbach, A. (1958) *Biochem. Prep.* 6, 83–90.
- Kessler, H., Griesinger, C., Zarbock, J., & Loosli, H. R. (1984) *J. Magn. Reson.* 57, 331–336.
- Knight, S., Andersson, I., & Brändén, C.-I. (1990) *J. Mol. Biol.* 215, 113–160.
- Kuehn, G. D., & Hsu, T.-C. (1978) *Biochem. J.* 175, 909–912.
- Larimer, F. W., Mural, R. J., & Soper, T. S. (1990) *Protein Eng.* 3, 227–231.
- Larimer, F. W., Harpel, M. R., & Hartman, F. C. (1994) *J. Biol. Chem.* 269, 11114–11120.
- Larson, E. M., Larimer, F. W., & Hartman, F. C. (1995) *Biochemistry* 34, 4531–4537.
- Lee, E. H., Harpel, M. R., Chen, Y.-R., & Hartman, F. C. (1993) *J. Biol. Chem.* 268, 26583–26591.
- Lilley, R. M., Riesen, H., & Andrews, T. J. (1993) *J. Biol. Chem.* 268, 13877–13884.
- Lorimer, G. H. (1981) *Annu. Rev. Plant Physiol.* 32, 349–383.
- Lorimer, G. H., & Andrews, T. J. (1973) *Nature* 243, 359–360.
- Lorimer, G. H., Andrews, T. J., & Tolbert, N. E. (1973) *Biochemistry* 12, 18–23.
- Lorimer, G. H., Chen, Y.-R., & Hartman, F. C. (1993) *Biochemistry* 32, 9018–9024.
- Marion, D., & Wüthrich, K. (1983) *Biochem. Biophys. Res. Commun.* 113, 967–974.
- Massey, V. (1994) *J. Biol. Chem.* 269, 22459–22462.
- Miziorko, H. M., & Lorimer, G. H. (1983) *Annu. Rev. Biochem.* 52, 507–535.
- Mogel, S. N., & McFadden, B. A. (1990) *Biochemistry* 29, 8333–8337.
- Morell, M. K., Paul, K., O'Shea, N. J., Kane, H., & Andrews, T. J. (1994) *J. Biol. Chem.* 269, 8091–8099.
- Newman, J., & Gutteridge, S. (1993) *J. Biol. Chem.* 268, 25876–25886.
- Ogren, W. L. (1984) *Annu. Rev. Plant Physiol.* 35, 415–442.
- Paech, C., Pierce, J., McCurry, S. D., & Tolbert, N. E. (1978) *Biochem. Biophys. Res. Commun.* 83, 1084–1092.
- Petersson, G. (1992) *Org. Mass Spectrom.* 6, 577–592.
- Pierce, J., Tolbert, N. E., & Barker, R. (1980) *Biochemistry* 19, 934–942.
- Pierce, J., Andrews, T. J., & Lorimer, G. H. (1986) *J. Biol. Chem.* 261, 10248–10256.
- Pigman, W. W., & Goep, R. M., Jr. (1948) *Carbohydrate Chemistry*, p 331, Academic Press, New York.
- Porter, M. A., Stringer, C. D., & Hartman, F. C. (1988) *J. Biol. Chem.* 263, 123–129.
- Robison, P. D., Martin, M. N., & Tabita, F. R. (1979) *Biochemistry* 18, 4453–4458.
- Schloss, J. V. (1990) in *Enzymatic and Model Carboxylation and Reduction Reactions for Carbon Dioxide Utilization* (Aresta, M., & Schloss, J. V., Eds.) pp 321–345, Kluwer Academic Publishers, Dordrecht, The Netherlands.
- Schloss, J. V., Phares, E. F., Long, M. V., Norton, I. L., Stringer, C. D., & Hartman, F. C. (1982) *Methods Enzymol.* 90, 522–528.
- Schreuder, H. A., Knight, S., Curmi, P. M. G., Andersson, I., Cascio, D., Sweet, R. M., Brändén, C.-I., & Eisenberg, D. (1993) *Protein Sci.* 2, 1136–1146.
- Selman, S., & Eastham, J. F. (1960) *Q. Rev., Chem. Soc.* 14, 221–233.
- Smith, H. B., & Hartman, F. C. (1988) *J. Biol. Chem.* 263, 4921–4925.
- Soper, T. S., Mural, R. J., Larimer, F. W., Lee, E. H., Machanoff, R., & Hartman, F. C. (1988) *Protein Eng.* 2, 39–44.
- Tapia, O., & Andrés, J. (1992) *Mol. Eng.* 2, 37–41.
- Tse, J. M.-T., & Schloss, J. V. (1993) *Biochemistry* 32, 10398–10403.
- Van Berkel, G. J., Glish, G. L., & McLuckey, S. A. (1990) *Anal. Chem.* 62, 1284–1295.
- Wray, J. W., & Abeles, R. H. (1995) *J. Biol. Chem.* 270, 3147–3153.

BI9508496